

### Contents lists available at ScienceDirect

# Polymer

journal homepage: www.elsevier.com/locate/polymer



# Designable phase structure in semi-interpenetrating polymer network (semi-IPN) materials: an idea to alter interfacial adhesion along the fibre in polymer composites

Balázs Magyar <sup>a</sup>, Tibor Czigány <sup>a,b</sup>, Gergő Zsolt Marton <sup>a,c</sup>, Fanni Balogh <sup>a,c</sup>, Gábor Szebényi <sup>a,c,\*</sup>

### ARTICLE INFO

### Keywords: Semi-IPN Interfacial shear strength 3D printing Pseudo-ductility

### ABSTRACT

The pseudo-ductile behaviour of carbon fibre-reinforced polymer composites can be enhanced through the integration of thermoplastic phases into the thermoset matrix. This study investigates the formation and control of phase morphology in epoxy resin modified with poly(ε-caprolactone) (PCL), targeting the development of a semi-interpenetrating polymer network (semi-IPN) structure. Phase morphology and thermal transitions were analysed using differential scanning calorimetry (DSC), atomic force microscopy (AFM), and scanning electron microscopy (SEM). The interfacial shear strength between the matrix and reinforcing fibres was evaluated through microdroplet testing. Furthermore, a novel strategy was introduced using 3D printing to locally modulate phase structure along the fibre length, offering spatial control over fibre–matrix interactions. The results demonstrate the feasibility of tuning composite interphases to improve toughness and interfacial behaviour in advanced structural materials.

# 1. Introduction

In recent years, attention has been paid to modifying matrix phases for developing tougher carbon fibre-reinforced composites. Enhancing the energy absorption capacity of the resin phase is a critical strategy to increase the damage tolerance and delay catastrophic failure in high-performance composites [1–4].

Due to their highly crosslinked molecular networks, thermosetting matrices are typically rigid and prone to rapid crack propagation. This limitation can be addressed—either locally or throughout the material—by incorporating various additives such as rubber particles or thermoplastic polymers. Systems composed of at least two different polymers are classified as polymer blends, which can further be categorised based on morphology and interfacial bonding into blends, graft copolymers, block copolymers, partially and fully interpenetrating polymer networks (IPNs), and crosslinked copolymers. In simple blends, the polymer components are physically mixed without chemical bonds,

whereas graft copolymers involve covalent bonding between phases, as exemplified by high-impact polystyrene (HIPS) [5–7]. IPNs are three-dimensional, entangled structures of at least two polymer networks, with molecular interpenetration that cannot be reversed without breaking covalent bonds [8,9].

The toughening of epoxy resin systems with thermoplastic polymers has been a research focus since the 1980s [10,11]. Unlike rubber-based modifiers, thermoplastics maintain the resin's strength and elastic modulus at relatively low loadings. Hendrick et al. [12] reviewed early advances in thermoplastic-based toughening agents. Yee and Pearson [13] highlighted four key parameters affecting toughening efficiency: particle size, particle stiffness, particle—matrix adhesion, and uniform dispersion. Murakami et al. [14] examined epoxy systems with varying crosslink densities and found that thermoplastic additives improved toughness more than rubber modifiers at high crosslink densities. Studies by Pearson et al. [15], Min et al. [16], and Gilbert et al. [17] using PPO, PSF, and PEI, respectively, demonstrated that increasing

E-mail address: szebenyi@pt.bme.hu (G. Szebényi).

a Department of Polymer Engineering, Faculty of Mechanical Engineering, Budapest University of Technology and Economics, Müegyetem rkp. 3., H-1111, Budapest,

<sup>&</sup>lt;sup>b</sup> HUN-REN-BME Research Group for Composite Science and Technology, Müegyetem rkp. 3., H-1111, Budapest, Hungary

<sup>&</sup>lt;sup>c</sup> MTA-BME Lendület Sustainable Polymers Research Group, Műegyetem rkp. 3., H-1111, Budapest, Hungary

<sup>\*</sup> Corresponding author. Department of Polymer Engineering, Faculty of Mechanical Engineering, Budapest University of Technology and Economics, Műegyetem rkp. 3., H-1111, Budapest, Hungary.

thermoplastic content improved the critical strain energy release rate (GIc), as the additives dissolved within the matrix and influenced phase morphology.

Depending on their constituents, IPN systems are classified as true IPNs, where both components are crosslinked, or semi-IPNs, in which only one component is crosslinked while the other remains thermoplastic. These hybrid matrix systems combine the advantageous properties of both components, similar to hybrid reinforcement concepts in composite design [10,18,19]. The rationale for combining PCL and epoxy lies in leveraging the toughness of thermoplastics with the stiffness of thermosets, aiming for synergistic improvements in composite performance. While PCL offers ductility and energy absorption, epoxy ensures high mechanical strength and thermal resistance. Their interaction can lead to tunable morphologies depending on curing conditions and blend ratios. IPNs are often treated as quasi-homogeneous systems, where phase separation is restricted by molecular-level physical entanglement and secondary bonding.

Karger-Kocsis [20] explored semi-IPNs formed by combining polycaprolactone (PCL) [21] with epoxy resins of differing glass transition temperatures. During curing, phase separation occurred, and semi-IPN morphology became increasingly evident at higher PCL concentrations. Above 50 wt% PCL, phase inversion was observed, with PCL forming the continuous matrix phase (confirmed via optical microscopy). Similarly, Grischuk et al. [22] demonstrated that adding PESU induced a dispersed second phase during curing, contributing to energy dissipation and enhanced toughness. They reported that lower molecular weight PESU formed fine, submicron domains, while high molecular weight PESU formed larger droplets. As a result, fracture toughness (Gc) improved by 20 % and 140 % for medium and high molecular weights, respectively, compared to unmodified epoxy (Gc = 151  $\pm$  21  $\rm J/m^2$ ).

Siddhamalli [23] showed that increasing PCL content in epoxy matrices enhanced energy absorption under impact loading. Lee et al. [24] used polysulfone (PES) as a second phase and observed significant improvements in mechanical performance at 25 wt% content, including a 44 % increase in tensile strength, a 35 % increase in impact strength, and an 11 % increase in fracture toughness. Qu et al. [25] and Liu et al. [26] studied partial-IPN systems with polyimide (PI) and epoxy, observing that even at 15 wt% PI, a continuous thermoplastic phase could form alongside clear phase separation, contributing to both toughening and thermal stability.

Nakanishi et al. [27] introduced the concept of gradient IPNs, where spatially controlled phase morphology is achieved by varying UV crosslinking intensity during curing. At lower intensities, dual continuous phases were observed, while higher UV exposure led to differential crosslinking rates and more complex morphologies.

Despite the extensive literature, the definition and identification of IPNs remain inconsistent. In many cases, systems exhibiting large-scale phase boundaries are referred to as IPNs, although their structure may more closely resemble blends. Moreover, the molecular-level entanglement required for a true IPN is often not verified experimentally. In semi-IPN studies, it is often assumed that thermoplastics dissolve into the epoxy matrix prior to curing. However, this assumption is increasingly questioned. Recent studies have shown that in systems with limited compatibility, phase separation and redistribution of thermoplastics-rather than full dissolution-are more likely to occur during the curing cycle (e.g., Refs. [15,22]). The extent of miscibility depends strongly on molecular weight, polarity, and thermal conditions during processing. The widespread assumption of homogeneous mixing before curing lacks empirical support, and in most cases, thermoplastic domains are likely dispersed rather than molecularly integrated. Thus, while many studies infer the presence of IPN or semi-IPN structures, their existence is rarely proven. This highlights the need for a methodology that enables the controlled creation and precise identification of phase structures, especially when such structures are leveraged to enhance mechanical performance.

This study aims to demonstrate a novel approach for the controlled formation of semi-interpenetrating polymer network (semi-IPN) structures within fibre-reinforced epoxy composites using 3D printing. By locally depositing polycaprolactone (PCL) via fused filament fabrication (FFF), we enable spatially resolved control over the thermoplasticthermoset interface during the curing process. This method provides a designable pathway to tailor interfacial adhesion along the reinforcement direction and to manipulate interlayer morphology. Through a combination of analytical techniques-including FTIR, Raman spectroscopy, DSC, DMA, AFM, SEM, and microdroplet shear tests-we explore the resulting phase behaviour, interfacial transitions, and mechanical implications of PCL content and processing. Our findings establish a foundation for engineering functionally graded interfaces that enable local modulation of fibre-matrix interactions, toughening mechanisms, and crack propagation behaviour in advanced structural composites.

### 2. Materials

The investigated epoxy matrix was composed of IPOX ER 1010 (IPOX Chemicals Kft., Budapest, Hungary), a DGEBA-based epoxy resin (EP), and IPOX MH 3111 amine-based curing agent. The mixing weight ratio was 100:75, as recommended by the manufacturer. The curing process for the EP was carried out at 90 °C. For the thermoplastic phase, eMorph175N05 poly( $\epsilon$ -caprolactone) (PCL) filament from Shenzhen Esun Industrial Co. Ltd. (Shenzhen, China) was used. The filament had a diameter of 1.75 mm, with a melting temperature (Tm) of 60 °C and a printing temperature of 180 °C. The fibre reinforcement investigated was PX35FBUD0300 unidirectional carbon weave (309 g/m² surface weight) from Zoltek Zrt. (Nyergesújfalu, Hungary), made of Panex35 50k rovings. Individual fibers were removed from this reinforcement structure for the microdroplet tests.

### 3. Manufacturing of the EP-PCL mixtures and specimens

To investigate the phase structure of the mixtures, epoxy resin–PCL mixtures were prepared with varying PCL content (ranging from 0 to 100 wt% in steps of 12.5 wt%). PCL was added to component A of the epoxy resin at 90 °C and placed in a drying oven for 1 h. The thermoplastic material was initially softened at 90 °C and then physically blended into the epoxy resin using a dry mixer for 10 min at moderate speed. This step aimed to achieve macroscopic dispersion rather than molecular-scale mixing, given the limited miscibility of the two phases. Visual homogeneity was ensured through repeated inspection and stirring prior to adding the curing agent. Component B of the resin system was subsequently added, and mixing continued for an additional 5 min. The prepared mixtures were poured into silicone moulds with cavity dimensions of 56  $\times$  13  $\times$  3 mm, and the samples were cross-linked at 90 °C for 3 h.

To examine the developed phases, polished slides of the samples were prepared. The mixtures were embedded in IPOX MR 3012 - MH 3122 epoxy resin and polished using a Struers Labopol-5 machine (15 min of wet polishing with K500, K1000, K2000, and K4000 sandpaper). After polishing, the surfaces were etched with dichloromethane to remove the thermoplastic phase. The samples were immersed in dichloromethane for 30 s, followed by soaking in acetone and distilled water for an additional 2 min to remove any residual dichloromethane.

For the microdroplet test, the same resin mixtures were used. Droplets of the mixtures were applied to individual carbon fibres, which were then cured at 90  $^{\circ}\text{C}$  for 3 h.

### 4. Experimental

### 4.1. Phase structure of the mixture

### 4.1.1. ATR-IR

The cured structure of the resin and thermoplastic material was first investigated using ATR-IR spectroscopy. Fig. 1 shows that the spectra of the mixtures exhibited simultaneous peaks characteristic of both base materials. These coincident intensity peaks were observed even at low PCL concentrations (25 wt%). For the epoxy resin samples, a sharp peak at 820 cm<sup>-1</sup> was observed, corresponding to the vibration of the aromatic carbon-hydrogen (C–H) bond, and a peak at 1500 cm<sup>-1</sup>, characteristic of the C—C skeleton vibration of the aromatic ring in DGEBA. These peaks were also present in the spectra of the mixtures, with their intensity decreasing as the PCL concentration increased.

For the PCL sample, two strong peaks, corresponding to the C–O–C stretching vibrations characteristic of aliphatic ester bonds, appeared at 1165 cm $^{-1}$  and 1240 cm $^{-1}$ . As the PCL concentration decreased, these peaks merged, resulting in a less distinct transition between them [28]. These peaks ultimately disappeared in the spectra of the epoxy resin samples. The peak at 1717 cm $^{-1}$ , typical of carbonyl group stretching, was also observed. For both reference samples, two peaks were visible at around 3000 cm $^{-1}$ : one at 2949 cm $^{-1}$ , corresponding to the asymmetric stretching of the  $^{-}$ CH $_2$  bond [29], and another at 2849 cm $^{-1}$ , due to the symmetric stretching of  $^{-}$ CH $_2$ . The intensity of these peaks remained unchanged in the mixtures.

The phase changes were closely monitored by magnifying the spectra between 1700 and 600 cm<sup>-1</sup> (Fig. 2). As the PCL concentration increases, the peaks characteristic of the epoxy resin appear in the mixture spectra, but their maximum absorbance values steadily decrease. This trend reverses when the PCL concentration decreases. For a 50 wt% PCL content, two peaks remain visible at 1140 and 1180 cm<sup>-1</sup>, with the latter corresponding to the vibrations of the aromatic ring [30]. However, as the PCL concentration increases, PCL becomes the dominant phase in the mixtures. A similar trend is observed at 1600 and 1503 cm<sup>-1</sup>, which correspond to the aromatic C=C bond characteristic of the DGEBA resin system, as well as at 800 cm<sup>-1</sup> (aromatic C-H) [31]. These signals are progressively smoothed out above 50 wt% PCL.

We also investigated the relationship between the phases using Raman spectroscopy on samples dissolved in dichloromethane. Dichloromethane is a solvent for PCL [32,33] and was used to examine the phase interaction in cross-linked samples. The samples were dissolved in a solvent bath at room temperature for 1 h, with the aid of an ultrasonic mixer (Bandelin Sonopuls 4200 HD). Fig. 3 shows that the intensity of the peaks characteristic of PCL decreased, as indicated by the

red-shaded regions (600–750 cm<sup>-1</sup>, 900–1050 cm<sup>-1</sup>, and 1220–1380 cm<sup>-1</sup>). This suggests that no first-order bonding between PCL and EP was formed during crosslinking. It is assumed that crosslinking of the epoxy component occurs independently for each phase, with the phases remaining completely separated during the process.

### 4.1.2. DSC

To further investigate the shift in the glass transition temperature (Tg) of PCL, DSC measurements were conducted on the samples. The change in the Tg of the epoxy resin phase was also observed in blends with higher PCL wt%. As shown in Fig. 4 and Table 1, the transition temperatures (PCL Tg, Tm, and EP Tg) shifted proportionally with increasing PCL mass fraction. No exothermic peak appeared in the mixture curves, indicating that the crosslinking of the epoxy resin occurred. Endothermic peaks, related to the melting of PCL, were observed in the blends. As the PCL content increased, the EP Tg shifted proportionally, consistent with the results of the DMA studies. The appearance of two distinct Tg peaks suggests incomplete mixing between the phases. Furthermore, the shift in EP Tg indicates that the addition of PCL softened the system, which may also contribute to a more ductile behaviour.

### 4.1.3. DMA

To further analyse the inter-phase relationship, dynamic mechanical analysis (DMA) tests were performed on samples with different epoxy resin–PCL concentrations. To ensure consistency, all DMA measurements were conducted under identical conditions (5 Hz frequency, 2  $^{\circ}$ C/min heating rate, three-point bending, from -75  $^{\circ}$ C to 125  $^{\circ}$ C). This ensured that trends in glass transition and modulus were attributable solely to composition changes, not thermal protocol differences. As the mass fraction of PCL increases, the loss modulus (E') decreases significantly at lower temperatures, with the temperature at which this decrease occurs approaching the Tm of PCL (Fig. 5).

A rubbery plateau does not occur in mixtures containing 62.5 wt% PCL, indicating that the system is already too annealed. Additional DSC measurements were performed to investigate the transition of the mixtures' Tg further. The rubbery plateau observed in mixtures with less than 62.5 wt% PCL suggests that a continuous epoxy resin phase remains present in the samples. The decrease in the rubbery plateau may indicate a phase inversion, where the epoxy resin no longer forms a continuous phase. Additionally, in this temperature range, PCL exists in a slurry state, which significantly increases segmental motion.

The distinct peak in tan  $\delta$  values may indicate good mixing and blending, while its decrease could suggest a reduction in crosslink density. At higher PCL concentrations (above 62.5 wt%), this peak falls

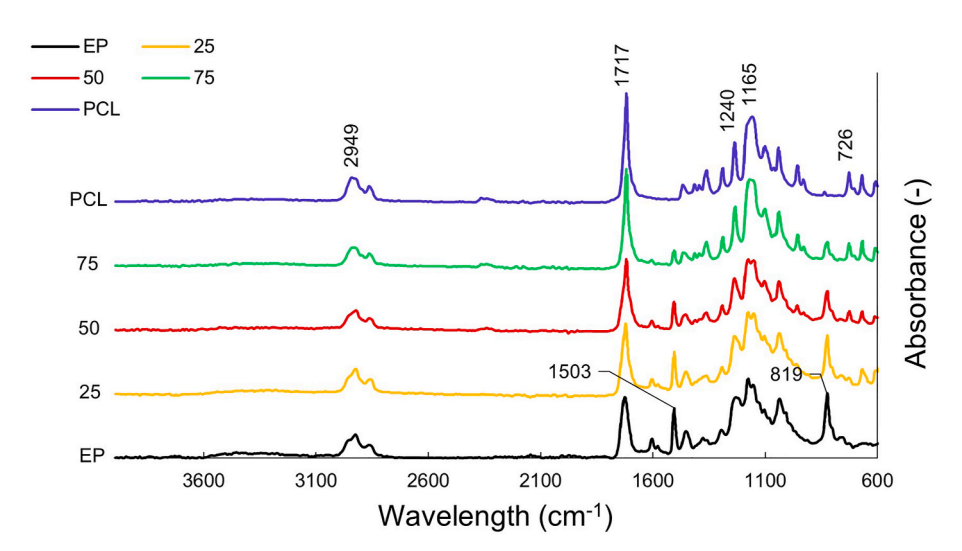


Fig. 1. FTIR spectra of epoxy resin-PCL mixtures with different wt% PCL content.

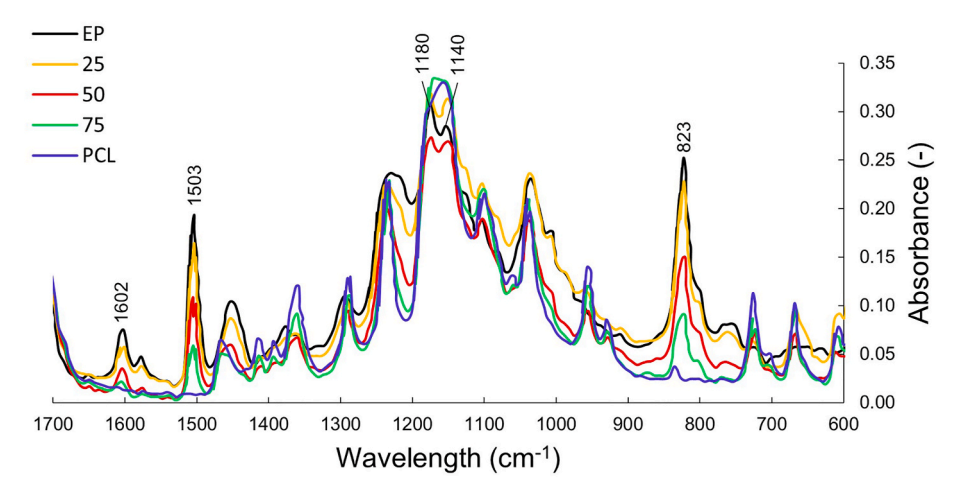


Fig. 2. FTIR spectra of epoxy resin-PCL mixtures with different wt% PCL content.

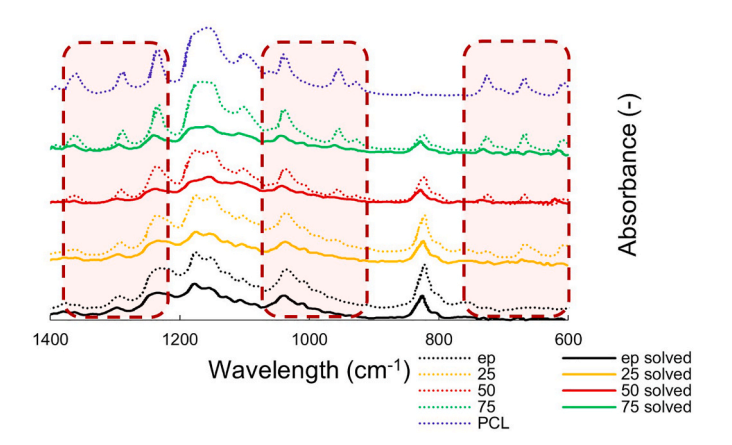


Fig. 3. FTIR spectra of dissolved PCL containing samples compared to their original/starting curves at different PCL wt% for epoxy resin/PCL mixtures.

below that of pure PCL (Fig. 5).

In the magnified plots of the DMA curves around the Tg of PCL (Fig. 6), it can be observed that the Tg characteristic of PCL increases as the additive concentration decreases. The transition temperature is also evident in the mixtures, even for samples containing 12.5 wt% PCL, although the peak appears shifted. This shift can be attributed to the fact that the Tg of epoxy resin is higher than that of PCL, and the transition

**Table 1**Transition temperatures for PCL/EP blends.

PCL wt%	Pcl Tg °C	pcl T <sub>m</sub> °c	EP Tg °C
0.0	_	_	82.3
12.5	-10.3	51.4	81.7
25.0	-31.4	53.1	80.3
37.5	-41.5	54.2	77.5
50.0	-45.4	54.9	73.3
62.5	-46.9	55.1	71.8
<i>75.0</i>	-48.7	55.2	68.8
87,5	-58.5	55.3	52.4
100	-65.7	60.6	-

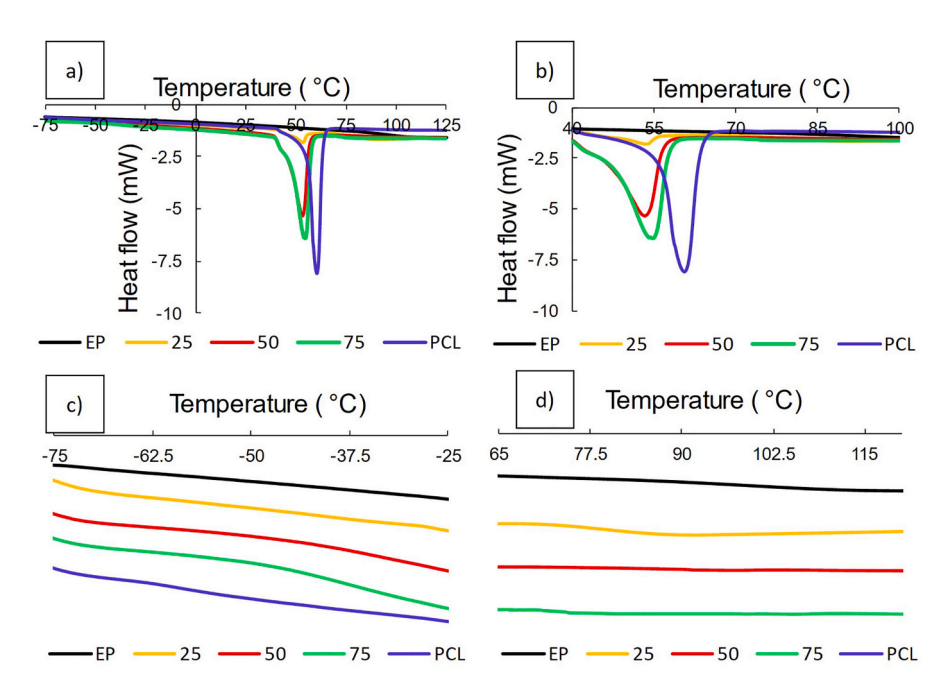


Fig. 4. DSC curves of PCL-EP mixtures; a) Full range; b) PCL at Tm and EP at Tg; c) Elongated curves around PCL at Tg; d) Elongated curves around EP at Tg.

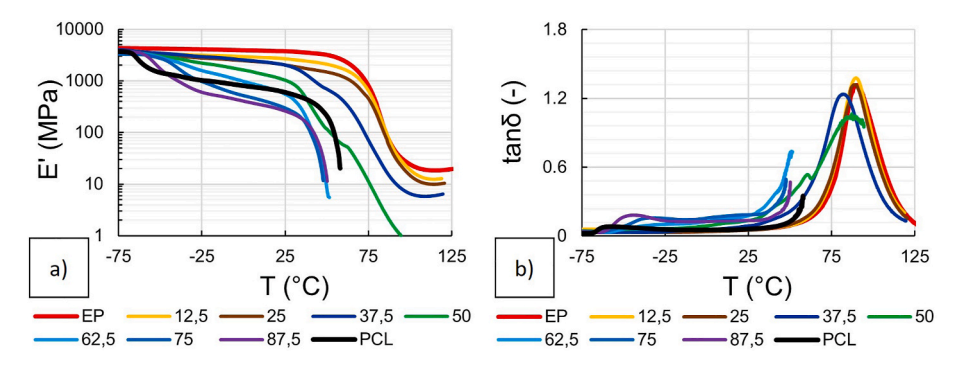


Fig. 5. DMA curves of different epoxy resin and PCL mixtures (in the explanations of the symbols, the numbers indicate the wt % of PCL); a) E' as a function of temperature; b)  $tan\delta$  as a function of temperature.

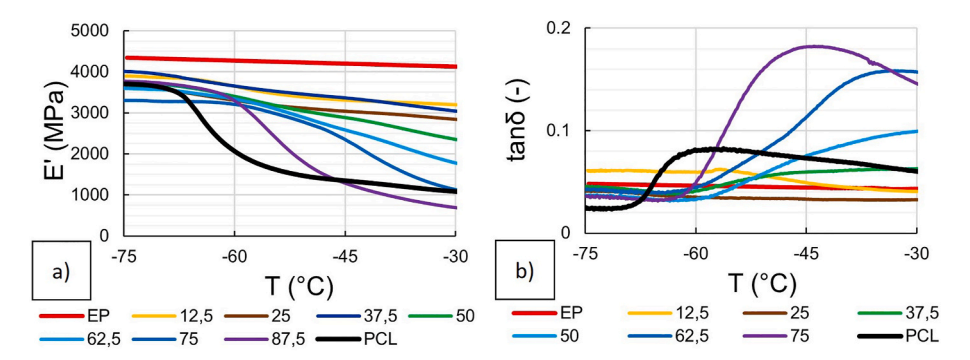


Fig. 6. DMA curves of different epoxy resin and PCL blends at Tg of PCL (numbers represent wt % of PCL); a) E' as a function of temperature; b)  $tan\delta$  as a function of temperature.

temperature of the mixture shifts towards that of the epoxy resin. The appearance of this peak suggests that PCL remains a continuous phase within the system.

Grischuk and Karger-Kocsis [34] studied the temperature shift of Tg in EP-VE IPN systems. They determined the degree of segregation ( $\alpha$ ) using the equation prescribed by Lipatov [35–37], which quantifies the compatibility of the constituents in the IPN system (1), where

$$\alpha = \frac{h_1 + h_2}{h_1^0 + h_2^0} \tag{1}$$

 $\alpha$  is the degree of segregation  $(-),\,h_1^0$  and  $h_2^0\,(-)$  are the tan\delta vs T curves of the component peaks at Tg for unmixed components,  $h_1$  and  $h_2\,(-)$  are the peaks appearing in the mixture samples at the Tg temperature of the components. If not only the tan value changes in the emerging peaks, then the temperature shifts should also be taken into account (2), where

$$\alpha = \frac{(h_1 + h_2) - (l_1 h_1 + l_2 h_2)/L}{h_1^0 + h_2^0}$$
 (2)

 $l_1$  and  $l_2$  (°C) are the offset values of the Tg peaks on the x-axis (temperature axis), and L (°C) is the temperature difference between the Tg peaks of the starting materials. The parameter  $\alpha$  can take values between 0 and 1. If  $\alpha$  is close to 0, complete phase separation is observed, while if  $\alpha$  is close to 1, complete mixing of the phases is seen.

Using equation (2), the degree of segregation can be determined, which indirectly characterises the relationship between the phases (Fig. 7). As the mass percentage of PCL increases, the segregation coefficient decreases, approaching 0, indicating that a co-continuous structure can form at higher PCL/EP ratios. In the figure, the regions where exact tan  $\delta$  values could not be determined are marked in red. However, the segregation coefficient values can still be estimated from the offset temperatures, based on the results from DSC measurements (i.

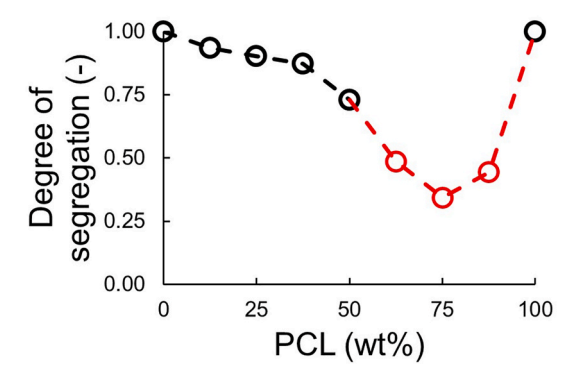


**Fig. 7.** Variation of degree of segregation as a function of PCL wt% based on DMA studies (for the red section using DSC results). (For interpretation of the references to colour in this figure legend, the reader is referred to the Web version of this article.)

e., by estimating tan  $\delta$  values of the peaks based on previous trends). This estimation was necessary because, above 50 wt% PCL, the samples were too annealed in the DMA apparatus, and the elastic portion of the EP Tg transition was no longer measurable. Nonetheless, the results indicate that a change in the interphase structure occurs in this region, as a decrease in the degree of segregation was observed even before reaching 50 wt% PCL.

# 4.1.4. AFM

AFM measurements were performed to gain additional insights into the emerging phases. For this, samples were first prepared using a microtome (Leica EM UC6, Wetzlar, Germany) with glass blades for sectioning. AFM imaging was conducted in intermittent contact (tapping) mode with a Nanosurf Flex AFM 5 device.

The phase structure between the epoxy resin and PCL was examined along the cross-section of the mixtures (Fig. 8). In Fig. 8(a), the darker and lighter phases appear uniformly, indicating a phase-separated structure. The darker regions correspond to the softer zones with higher attenuation, which, in this case, are the PCL zones, while the lighter, whiter regions correspond to the epoxy resin phase with lower attenuation. For the 25 wt% PCL samples, the darker PCL phases are smaller in size compared to those in the 50 wt% samples; however, in both cases, the phases are uniformly distributed across the image. In the 75 wt% PCL samples, larger islands of phases form, with the darker PCL phase, exhibiting higher attenuation, being dominant. These measurements suggest that between 50 and 75 wt% PCL, a phase inversion may occur, in which the roles of the epoxy resin and PCL phases in the inclusion matrix may switch. The images also reveal that the cross-section is not homogeneous, with different shades appearing, which supports the idea of phase separation during crosslinking. However, the images do not provide conclusive evidence as to whether these phases are biphasic or whether one phase is dispersed and the other continuous.

### 4.1.5. SEM

To examine the phase structures, we used the previously etched and polished samples for SEM analysis. Samples with PCL contents ranging between 50 and 75 wt% were also tested, with the PCL content increased in 6.25 wt% increments. The SEM images of the etched samples are shown in Fig. 9.

It was observed that between 25 and 56.25 wt% PCL, the leached PCL exists as a dispersed phase within the system. However, as the PCL concentration increases to 62.5 wt%, a biphasic phase structure forms, replacing the previous dispersed phase structure (where PCL droplets were dispersed in the epoxy resin phase). With further increases in PCL

content, the epoxy resin phase forms smaller islands, as shown in Fig. 9 (d). In this case, PCL takes on the role of the encapsulating matrix, and phase inversion occurs. Finally, in Fig. 9(e), the epoxy resin phase is seen as dispersed droplets.

To better visualize the emerging phase structure, additional images were created using image editing software by adjusting the contrast levels. These images are presented in Fig. 10, where PCL is highlighted in green and the epoxy resin (EP) phases in yellow (for samples with 56.25–75 wt% PCL). It can be observed that as the PCL ratio increases, PCL takes over the role of the embedding matrix between 68.75 and 75 wt% PCL, indicating a phase inversion. Furthermore, the co-continuous phase around 62.5 wt% PCL is more clearly observed in the contrast-adjusted images. Contrast-enhanced images reveal the progression of morphology and help visualize phase continuity and inversion, supporting the interpretation of a co-continuous structure at intermediate PCL levels.

The SEM and AFM results jointly reveal a progressive morphological transition from dispersed domains to a co-continuous network as PCL content increases beyond 62.5 wt%. While domain sizes were not quantitatively measured, visual inspection across images shows increasing interconnectivity, especially in contrast-enhanced SEM at 62.5–75 wt%. This co-continuity supports the hypothesis of semi-IPN behaviour at the mesoscale, although no direct evidence of molecular entanglement (true IPN) was observed.

Phase morphology was analysed from SEM micrographs using a custom Python tool based on OpenCV and scikit-image. Grayscale images were binarized using Otsu's method, and the brighter (A-phase) regions were segmented (Fig. 11). Circular domains were detected, and their geometric features were quantified. The circularity of each detected phase region was computed using formula (3)

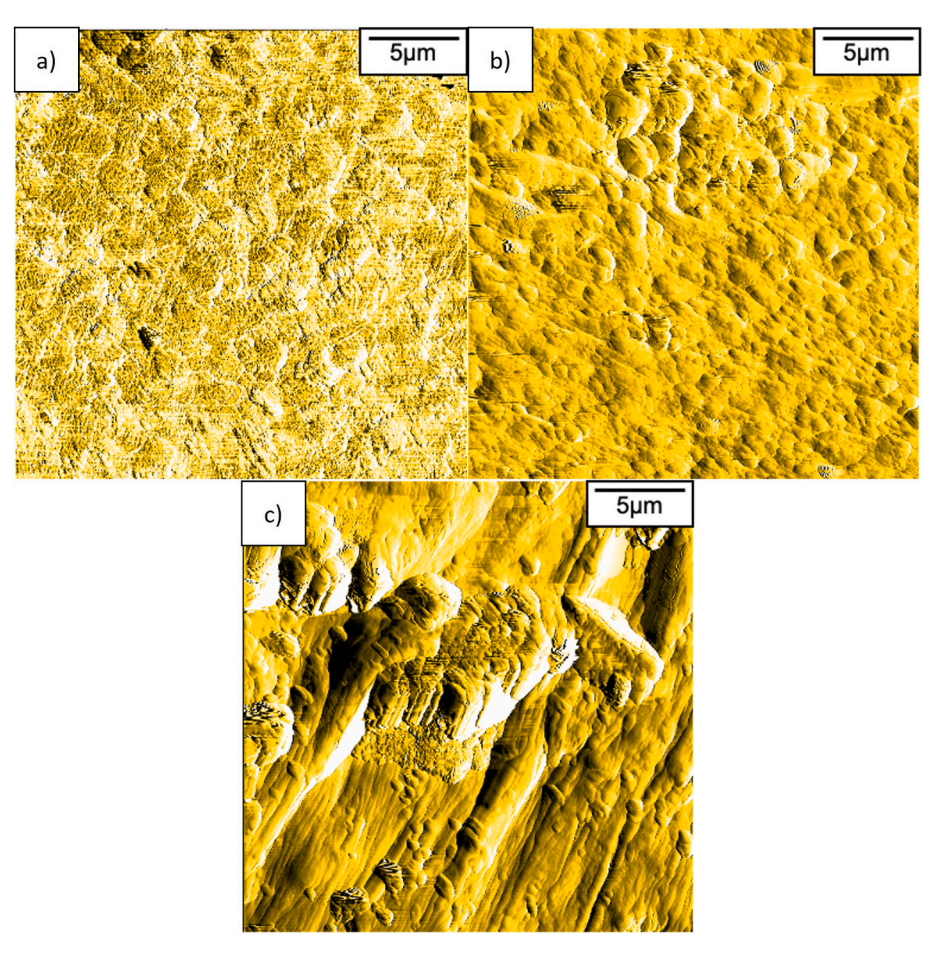


Fig. 8. Atomic force microscopy images; a) 25 wt%; b) 50 wt%; c) epoxy resin-PCL blends containing 75 wt% PCL.

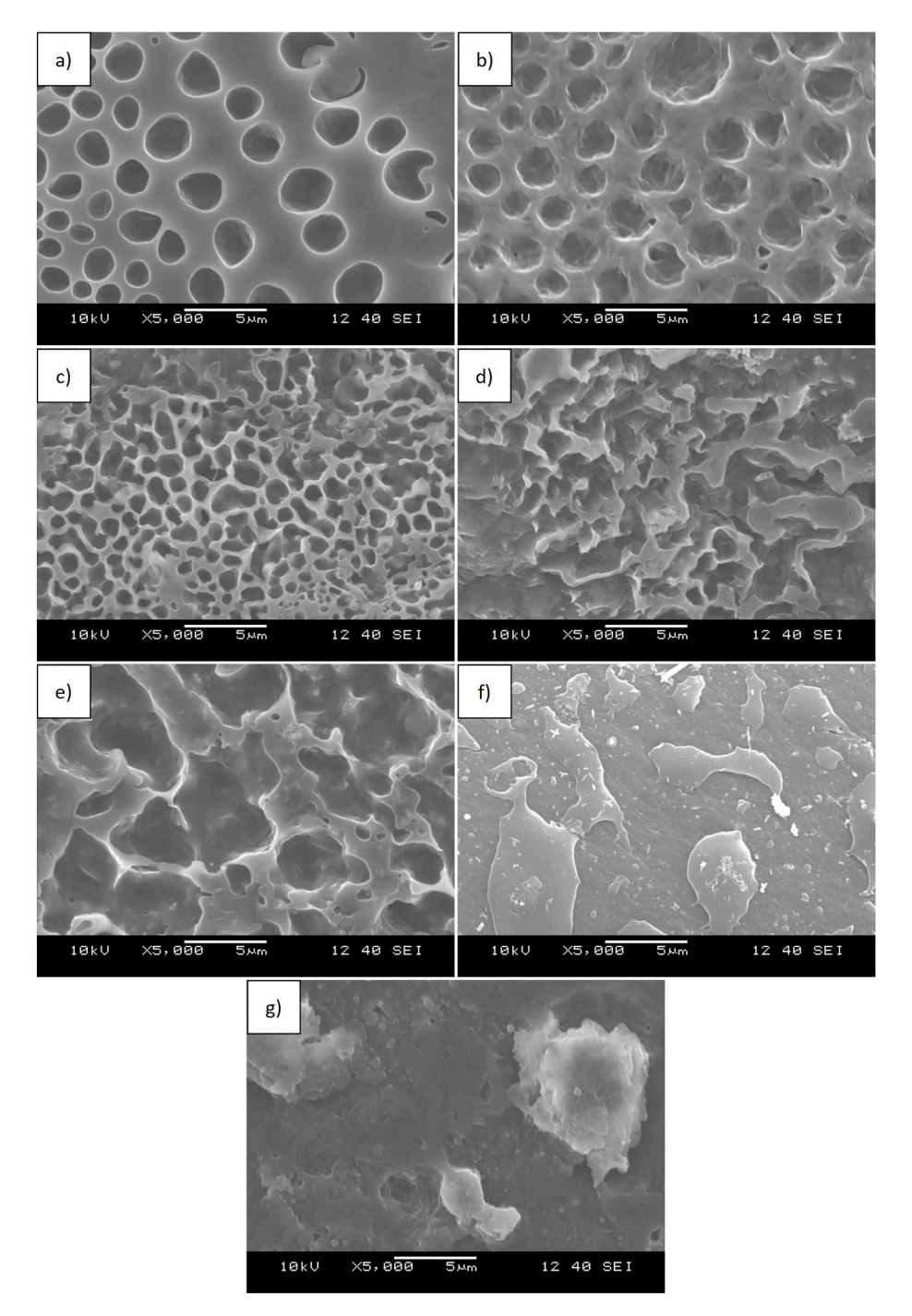


Fig. 9. SEM images of the etched surface of samples at 5000x magnification with different PCL content; a) 25 m%; b) 50 m%; c) 56.25 m%; d) 62.5 m%; e) 68.75 m%; f) 75 m%; g) 87.5 m%.

$$Circularity = \frac{4\pi \cdot A}{p^2} \tag{3}$$

where C is the circularity, A is the area (i.e., the number of pixels enclosed by the boundary of the region), and P is the perimeter (i.e., the number of pixels forming the boundary of the region). This dimensionless metric yields 1 for a perfect circle, and values less than 1 for increasingly irregular or elongated shapes. The constant  $4\pi$  normalizes the result so that the maximum circularity is 1, while squaring the perimeter ensures the units are consistent with area. Circularity thus provides a compactness measure of individual phases, with lower values indicating more complex or fragmented structures.

At lower PCL contents (<50 wt%), the PCL phase appears as

dispersed, nearly spherical domains within an EP matrix, resulting in higher circularity values for PCL (Fig. 12.). As the PCL content increases (62.5–68.75 wt%), both phases exhibit reduced circularity and increased variability, indicating the onset of a co-continuous morphology where neither phase is fully dominant and both forms interconnected networks. Beyond 75 wt% PCL, EP becomes the dispersed phase within a continuous PCL matrix, with EP showing higher circularity values due to its more isolated domain structure.

To further evaluate the microstructural evolution of the blends, the number of discrete polymer phases was quantified from SEM images using our segmentation-based image analysis tool. The resulting curve of detected phase counts as a function of PCL content is shown in Fig. 13. Interestingly, the data exhibit a pronounced non-linear trend: the

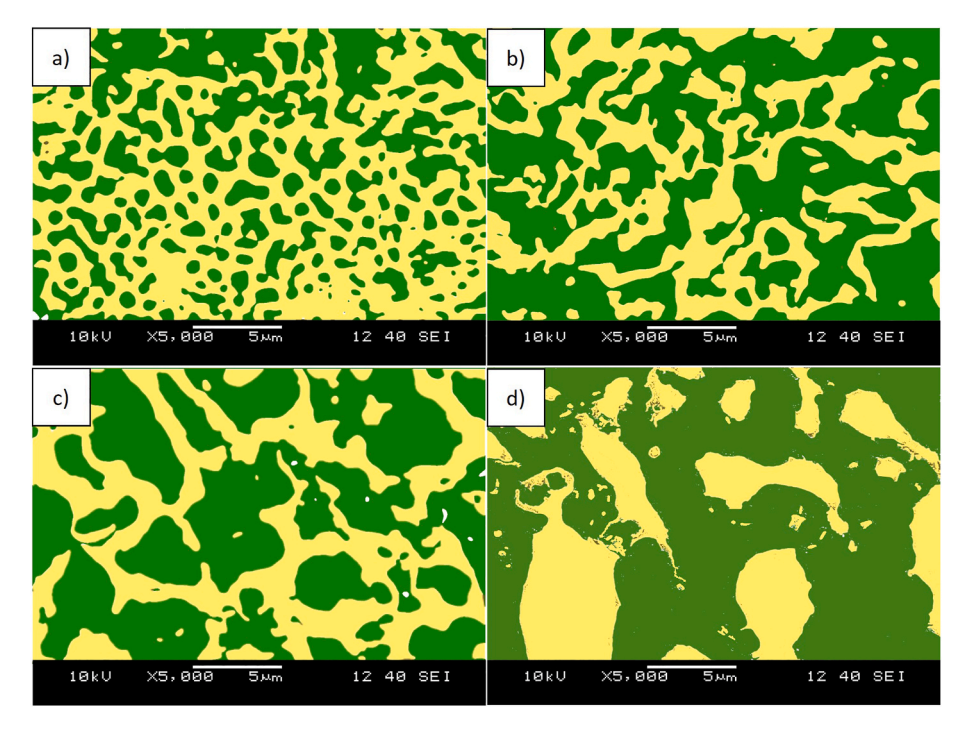


Fig. 10. Contrast images (phases are coloured for better visualisation, yellow = EP, green = PCL); a) 56.25 wt%; b) 62.5 wt%; c) 68.75 wt%; d) 75 wt%. (For interpretation of the references to colour in this figure legend, the reader is referred to the Web version of this article.)

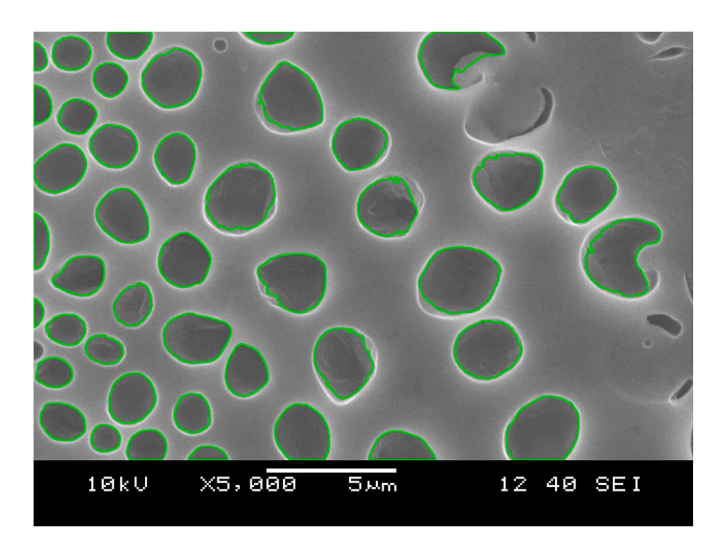


Fig. 11. Analysed SEM image in Python at 25 m% PCL content.

number of distinct domains increases gradually between 25 and 50 wt% PCL, but then spikes sharply at 56.25 wt%, followed by a steep decline from 62.5 wt% onward.

This sharp maximum in phase count at 56.25 wt% PCL suggests a critical compositional threshold, beyond which the phase morphology undergoes a transition from a dispersed to a co-continuous structure. The increase in domain count at this point indicates that the blend reaches a maximum interfacial area, characterized by the fragmentation of one phase into finely dispersed domains. Such a spike is characteristic of immiscible polymer blends nearing phase inversion or co-continuity, where both components approach similar volume fractions and begin forming interpenetrating networks.

This morphological signature aligns well with the thermal and mechanical transitions identified in the DSC and DMA analyses, which also pointed to a compositional window around 50–60 wt% PCL where the system transitions into a semi-interpenetrating polymer network (semi-

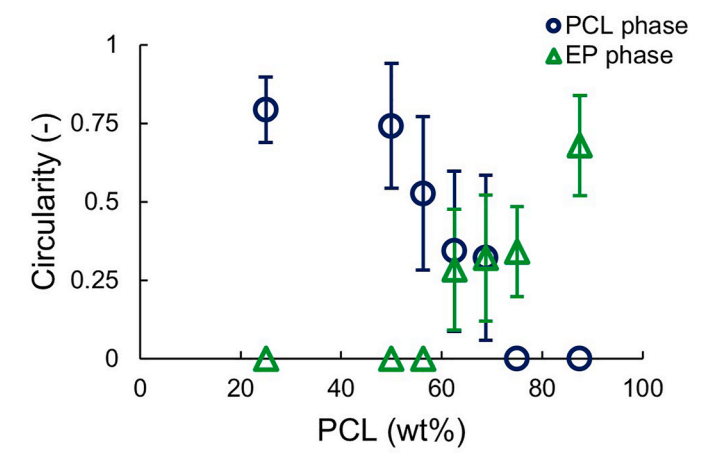


Fig. 12. Circularity of PCL and EP phases as a function of PCL content (wt%).

IPN). At this critical ratio, both the PCL and epoxy phases contribute significantly to the structural matrix, resulting in enhanced mechanical synergy and complex phase architecture.

Furthermore, the observed drop in average circularity and increase in the number of smaller, irregular domains at 56.25 wt% support the conclusion that the system reaches peak phase complexity and fragmentation at this composition. This transient morphology likely precedes the coalescence or inversion process, which becomes evident as the PCL content increases beyond 62.5 wt%, where the number of detected regions drops to near unity, indicating a transition to a continuous PCL matrix with embedded epoxy resin.

# 4.2. Microdroplet test

In many studies, blend systems are primarily examined by analysing the mixture of resin and thermoplastic materials, focusing on their potential curability and the resulting material structure. However, in the case of composites, the altered composite matrix may exhibit distinct

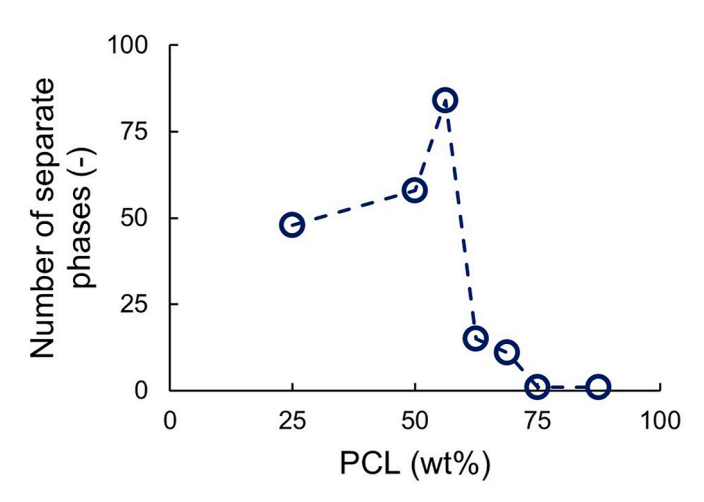


Fig. 13. Number of separate PCL phases in the mixtures a function of PCL content (wt%).

characteristics. For phases at the interface, the shear strength between the fibre and the matrix along the fibre length may vary locally, which in turn could influence the critical fibre length as the thermoplastic content changes.

Micro-droplet shear strength measurements were conducted to assess the interfacial shear strength. The test speed was set to 2 mm/min, with a shear blade spacing of 30  $\mu$ m. This setup allowed the carbon fibre to move freely between the blades, facilitating the deposition of droplets onto the blades. For each measurement, a matrix droplet was placed on an individual carbon fibre, and as the test proceeded, the droplet was wound onto the blades. Shear forces were applied at the fibre-matrix interface, and the fibre embedded in the droplet was progressively pulled out at the appropriate force. A total of 30 samples per test group were prepared. Based on the maximum force, fibre diameter, and embedded fibre length, the interfacial shear strength, and from this, the critical fibre length, were calculated using equation (4),

$$\tau = \frac{F_c}{\pi \cdot d_f \cdot L} \tag{4}$$

where t is the interfacial shear strength (MPa),  $F_c$  is the maximum force (N),  $d_f$  is the diameter of the fibre (mm), and L is the embedded length of the fibre (mm). The dimensions of the droplet and fibre were determined using optical microscopy. A reference pure epoxy resin matrix, along with resin mixtures containing varying PCL mass concentrations, was used for the tests. Matrix droplets were applied to the fibres from the prepared mixtures using a hypodermic needle, and the droplets were then cross-linked at 90 °C for 3 h in a drying oven.

The shear strength was found to significantly change with increasing PCL concentration (ANOVA test,  $P=95\,\%,\,n=179$ ). For PCL concentrations above 0.2 wt%, the shear strength decreased significantly compared to the reference sample (two-sample T-test,  $P=95\,\%,\,n=58$ ), as shown in Fig. 14. At PCL concentrations greater than 0.2 wt%, PCL phases began to appear at the interface, significantly weakening the matrix-fibre contact. The reduced interfacial shear strength results in a locally varied load transfer, potentially creating zones that could alter crack propagation behaviour. Note that although interfacial shear strength was only measured for low PCL contents, higher concentrations were studied to identify phase inversion behavior relevant to structural design.

# 4.3. Designable phase structure

In our previous research [38–40], the relationship between fibrous reinforcement and co-continuous systems has been shown to vary along the length of the fibers. PCL offers the potential for designing a

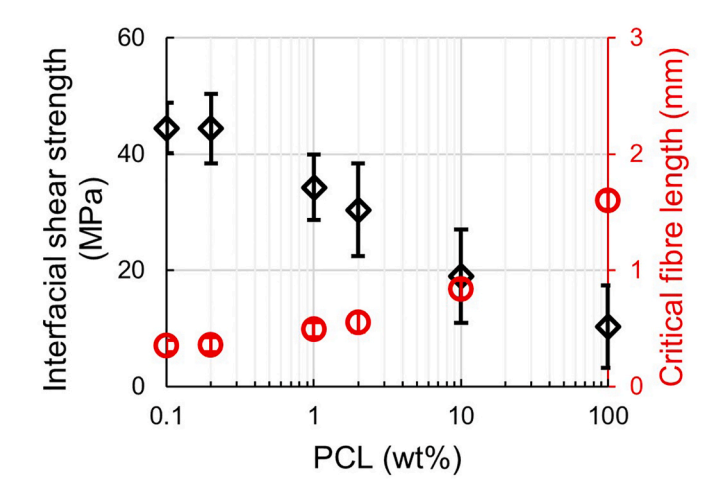


Fig. 14. Interfacial shear strength results on treated fibres measured by microdroplet tests.

customizable interface arrangement through Fused Filament Fabrication (FFF) printing. Using 3D printing, the thermoplastic material can be applied to the surface of the reinforcing fibers, where it can locally form a transition phase with the epoxy resin during crosslinking, creating the phase structure described above. This approach provides significant design flexibility, enabling designers to control the interface properties.

In our previous work, we used a stem mixer to disperse the thermoplastic material within the epoxy resin. However, in composite manufacturing, this type of mixing is not available. Typically, a static system is employed, where no external mixing is applied, and the matrix material is infused under vacuum. In this scenario, PCL phases are surrounded by the epoxy resin. It is important to determine whether mixing between the phases occurs during the resin's crosslinking process. If mixing does not occur, distinct phase boundaries between the thermoplastic and epoxy resin will form, which could become potential failure points.

For the tests, a PCL strip with a thickness of 0.4 mm and a width of 2 mm was fabricated using a 3D printer. The printed strip was then surrounded by epoxy resin and cured at 90  $^{\circ}$ C for 3 h (Fig. 15).

We investigated the distribution of the resulting phases using AFM. It was immediately apparent to the naked eye that the originally printed strip became distorted during the crosslinking process, with no sharp transition between the phases along the printed edges. This distortion occurred due to crosslinking temperatures exceeding the melting point (Tm) of PCL. AFM images further confirmed that the phase boundaries were not sharply defined; instead, a gradual transition between the phases was observed (Fig. 16), with both dark and light zones appearing in the images. This suggests that a smooth transition formed around the printed pattern during the resin crosslinking process, rather than a

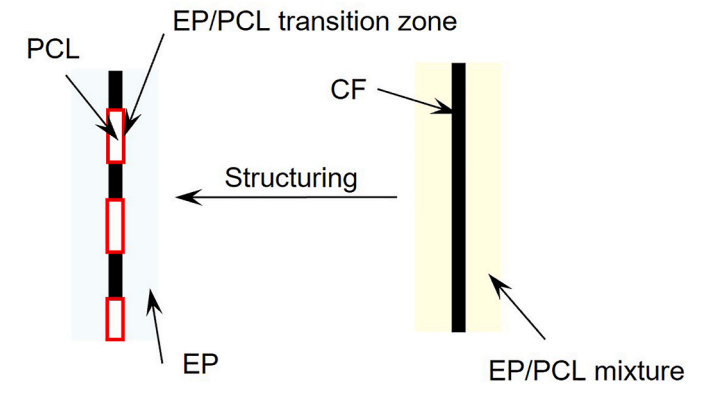


Fig. 15. The idea to design the phase structure around the fibre length.

completely distinct phase boundary. AFM line scans across the printed PCL—epoxy boundary show a gradual rather than sharp phase transition, supporting the concept of locally tunable morphology.

As in previous experiments, we polished the resulting phase structure, treated the surface with the PCL solvent for 2 min, then immersed the sample in an acetone bath, and finally placed it in distilled water for another 3 min. The SEM image obtained is shown in Fig. 17. It can be observed that the phases typical of the images in Fig. 10 are present simultaneously. Moving away from the EP phase, the size of the released PCL phases increases steadily. A small region of the co-continuous phase appears, followed by a phase inversion, where the EP phase appears as dispersed droplets. These observations are consistent with the AFM images. The SEM image captures a continuous transition from epoxydominated to PCL-dominated regions, reinforcing the possibility of engineered gradient morphologies.

Contrast-enhanced images reveal the progression of morphology and help visualize phase continuity and inversion, supporting the interpretation of a co-continuous structure at intermediate PCL levels (Fig. 18). Contrary to what is often reported in the literature, a co-continuous phase only formed within a specific range of PCL concentrations. In most cases, one phase appears as dispersed droplets within the other. In our study, the phase transition occurred between 60 and 70 wt% PCL, where a co-continuous phase transition was observed. To enhance visibility, we also created contrast images from the data shown in Fig. 18, where the phases were color-coded. Moving away from the initial EP phase, it can be observed that PCL initially appears as dispersed droplets within the EP matrix. After a short transition, PCL assumes the role of the embedding matrix in the system.

We conducted phase analysis based on both circularity and the number of separate domains in the printed patterned epoxy-PCL specimen. As shown in Fig. 17, the SEM image was divided into five equal zones from bottom to top to examine morphological variation across the cross-section. In the bottom region (Zone 1), where epoxy resin is dominant, only a small amount of dispersed PCL is present, resulting in fewer domains with relatively high circularity. Moving upward into Zone 2, the local concentration of PCL increases, leading to a sharp rise in the number of phases, closely resembling the trend observed in the 56.25 wt% PCL blend. In Zone 3, the number of domains begins to

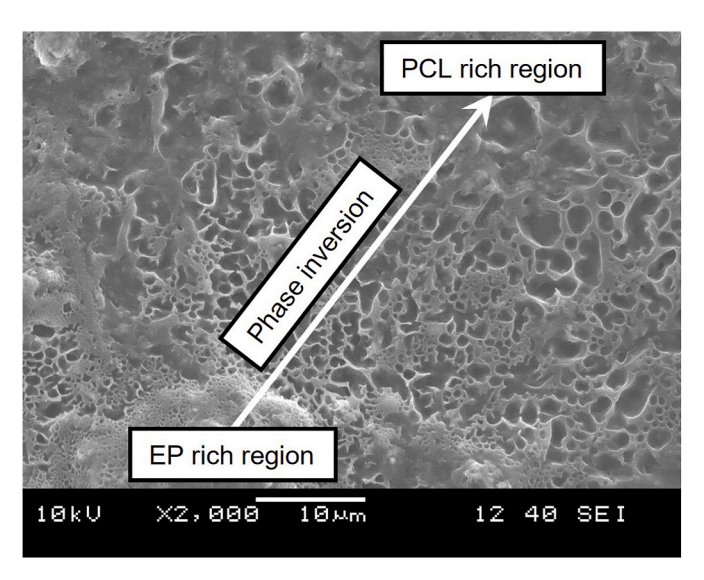


Fig. 17. Gradient-like phase structure around a printed pattern.

decline, suggesting the onset of phase coalescence or structural inversion. Finally, in Zones 4 and 5, the PCL phase becomes dominant, accompanied by a further reduction in both phase count and circularity.

This spatial variation in morphology provides physical evidence of a gradient in local phase composition, which closely mirrors the compositional transitions observed in the blend series. The observed peak in phase count at intermediate regions reinforces the interpretation of a cocontinuity threshold—where both epoxy and PCL form interpenetrating networks—before the system transitions into a PCL-dominated matrix (Fig. 19).

# 5. Conclusions

This study demonstrated a method for spatially controlled phase structuring in epoxy–PCL semi-interpenetrating polymer networks (semi-IPNs), leveraging 3D printing to locally tune interfacial adhesion.

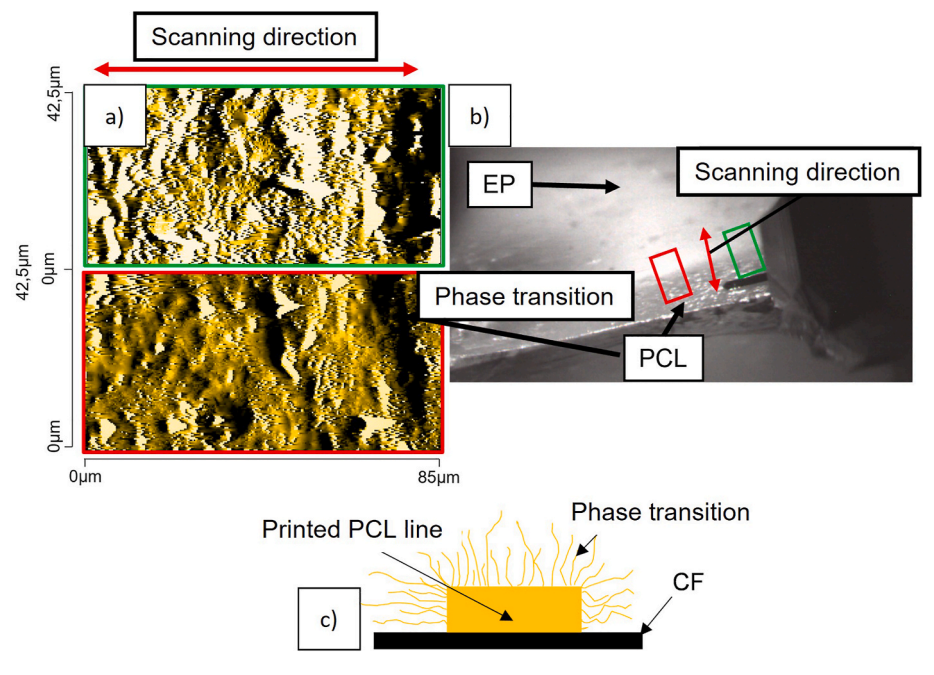


Fig. 16. a) AFM images of the phase transition between the printed pattern and the epoxy resin, AFM image based on line scans for a given colour (windows enlarged); b) AFM head scan between the printed pattern and the epoxy resin; c) Schematic diagram of the interlocking around the printed pattern. (For interpretation of the references to colour in this figure legend, the reader is referred to the Web version of this article.)

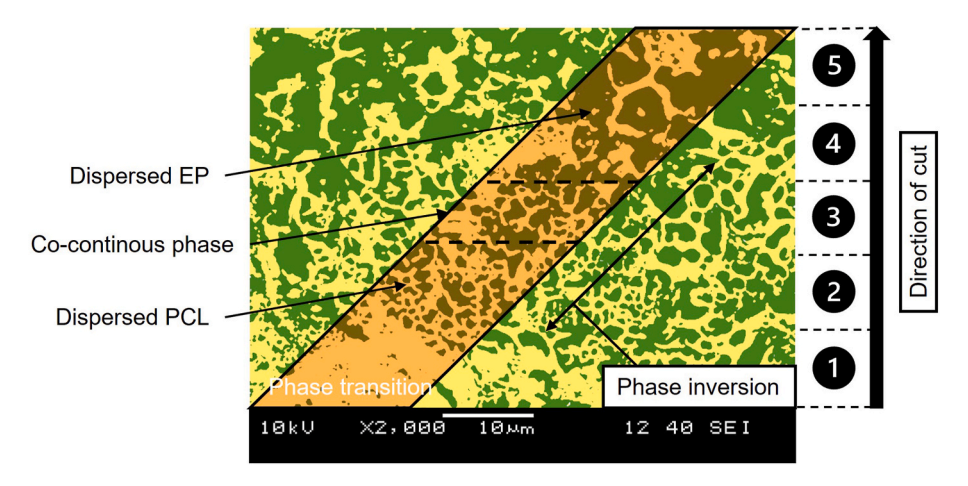


Fig. 18. Contrast image of the phase structure around the printed pattern with later analysis cuts definitions.

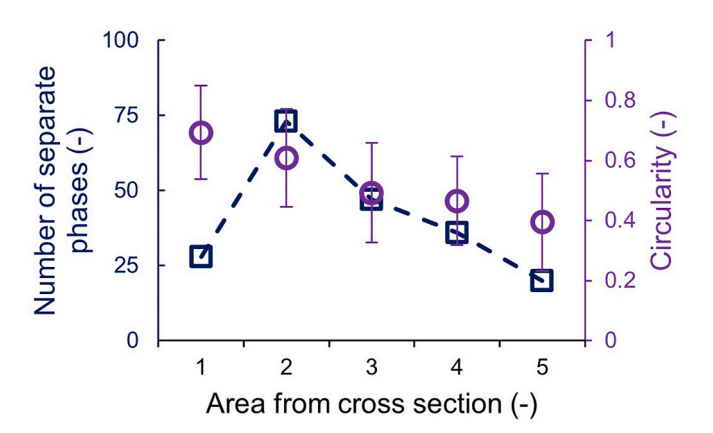


Fig. 19. Number of separate PCL phases and their circularity around the printed PCL in the specific zones from 1 to 5 (bottom to top).

We first analysed the phase structures formed in various epoxy resin and thermoplastic material mixtures. Using 3D printing, we created structured IPN zones within the resin, allowing us to locally modify the interfacial shear strength between the resin and reinforcing fibres, as well as alter interlayer contacts by introducing printed interlayers. Through this approach, we simultaneously enhanced the ductility of the matrix with thermoplastic material, applied interlayer technology via 3D printing, and reduced the likelihood of fibre breakage by adjusting the interfacial shear strength. Through phase characterization (DSC, SEM, AFM), we identified a transition to co-continuous morphology between 62.5 and 75 wt% PCL. This phase inversion region represents a design window for locally modifying interfacial shear strength, confirmed by microdroplet testing. The feasibility of integrating 3Dprinted PCL inserts into composite manufacturing was explored, suggesting compatibility with techniques such as vacuum infusion or hand lay-up. This strategy opens new possibilities for tailoring fibre-matrix interactions in structural composites.

## CRediT authorship contribution statement

Balázs Magyar: Writing – original draft, Methodology, Investigation, Conceptualization. Tibor Czigány: Writing – review & editing, Writing – original draft, Supervision, Conceptualization. Gergő Zsolt Marton: Writing – review & editing, Writing – original draft, Investigation. Fanni Balogh: Writing – review & editing, Writing – original draft, Investigation. Gábor Szebényi: Writing – review & editing, Writing – original draft, Methodology, Investigation, Funding acquisition, Conceptualization.

### **Declaration of competing interest**

The authors declare that they have no known competing financial interests or personal relationships that could have appeared to influence the work reported in this paper.

### Acknowledgements

We would like to sincerely thank the late Prof. Dr. h.c. mult. József Karger-Kocsis, for his support and valuable comments, which serve as a solid foundation for our research. The research has been supported by the NRDI Office (OTKA FK 142540). Gábor Szebényi acknowledges the financial support received through the János Bolyai Scholarship of the Hungarian Academy of Sciences and UNKP-23-5-BME-415 New National Excellence Program. Project no. 2022-2.1.1-NL-2022-00012 National Laboratory for Cooperative Technologies has been implemented with the support provided by the Ministry of Culture and Innovation of Hungary from the National Research, Development, and Innovation Fund, financed under the National Laboratories funding scheme. Project no. TKP-6-6/PALY-2021 has been implemented with the support provided by the Ministry of Culture and Innovation of Hungary from the National Research, Development and Innovation Fund, financed under theTKP2021-NVA funding scheme. Project no. KDP-IKT-2023-900-I1-00000957/0000003 has been implemented with the support provided by the Ministry of Culture and Innovation of Hungary from the National Research, Development and Innovation Fund, financed under the KDP-2023 funding scheme. The project supported by the Doctoral Excellence Fellowship Programme (DCEP) is funded by the National Research Development and Innovation Fund of the Ministry of Culture and Innovation and the Budapest University of Technology and Economics.

# Data availability

Data will be made available on request.

### References

- [1] G.Z. Marton, G. Szebényi, Influencing the damage process and failure behaviour of polymer composites – a short review, Express Polym. Lett. 19 (2025) 140–160.
- [2] M. Kuyumcu, C. Kurtulus, M. Ciftci, M.A. Tasdelen, Improving the mechanical properties of fiber-reinforced polymer composites through nanocellulose-modified epoxy matrix, Express Polym. Lett. 18 (2024) 61–71.
- [3] Szebényi Marton, Influencing the damage process and failure behaviour of polymer composites – a short review, Express Polym. Lett. 19 (2025) 140–160.
- [4] M.L. Vas, T. Czigány, P. Tamás-Bényei, Development of a new method for characterize resistance to cyclic tensile load in Mono and hybrid composites, Period. Polytech. - Mech. Eng. 69 (2) (2025) 93–102.
- [5] D.A. Thomas, L.H. Sperling, Chapter 11 interpenetrating polymer networks, in: D. R. Paul, S. Newman (Eds.), Polymer Blends, Academic Press, 1978, pp. 1–33.

- [6] P.F. Rempp, P.J. Lutz, 12 synthesis of graft copolymers, in: G. Allen, J. C. Bevington (Eds.), Comprehensive Polymer Science and Supplements, Pergamon, Amsterdam, 1989, pp. 403–421.
- [7] C. Hagiopol, Copolymers. Reference Module in Materials Science and Materials Engineering, Elsevier, 2016.
- [8] T.R. Hoare, D.S. Kohane, Hydrogels in drug delivery: progress and challenges, Polymer 49 (8) (2008) 1993–2007.
- [9] M.Q. Zhang, Reversibly interlocked polymer networks: a technology that can do more than eliminating phase separation in polyblends, Express Polym. Lett. 18 (2024) 559–560.
- [10] U. Farooq, J. Teuwen, C. Dransfeld, Toughening of epoxy systems with interpenetrating polymer network (IPN): a review, Polymers (2020).
- [11] J.H. Hodgkin, G.P. Simon, R.J. Varley, Thermoplastic toughening of epoxy resins: a critical review, Polym. Adv. Technol. 9 (1) (1998) 3–10.
- [12] J.L. Hedrick, I. Yilgor, M. Jurek, J.C. Hedrick, G.L. Wilkes, J.E. McGrath, Chemical modification of matrix resin networks with engineering thermoplastics: 1. Synthesis, morphology, physical behaviour and toughening mechanisms of poly (arylene ether sulphone) modified epoxy networks, Polymer 32 (11) (1991) 2020–2032.
- [13] A.F. Yee, R.A. Pearson, Toughening mechanisms in elastomer-modified epoxies, J. Mater. Sci. 21 (7) (1986) 2462–2474.
- [14] A.I.T. Murakami, D. Saunders, H. Aoki, T. Yoshiki, S. Murakami, O. Watanabe, M. Saito, H. Inoue, Proceedings of the Benibana International Symposium on Polymer Toughening, Yamagata, Japan, 1990, p. 65.
- [15] R.A. Pearson, A.F. Yee, Toughening mechanisms in thermoplastic-modified epoxies: 1. Modification using poly(phenylene oxide), Polymer 34 (17) (1993) 3658–3670.
- [16] B.G. Min, J.H. Hodgkin, Z.H. Stachurski, Reaction mechanisms, microstructure, and fracture properties of thermoplastic polysulfone-modified epoxy resin, J. Appl. Polym. Sci. 50 (6) (1993) 1065–1073.
- [17] A.H. Gilbert, C.B. Bucknall, Epoxy resin toughened with thermoplastic, Makromol. Chem., Macromol. Symp. 45 (1) (1991) 289–298.
- [18] M.A. Haque, T. Kurokawa, J.P. Gong, Super tough double network hydrogels and their application as biomaterials, Polymer 53 (9) (2012) 1805–1822.
- [19] P. Matricardi, C. Di Meo, T. Coviello, W.E. Hennink, F. Alhaique, Interpenetrating polymer networks polysaccharide hydrogels for drug delivery and tissue engineering, Adv. Drug Deliv. Rev. 65 (9) (2013) 1172–1187.
- [20] J. Karger-Kocsis, Self-healing properties of epoxy resins with poly(ε-caprolactone) healing agent, Polym. Bull. 73 (11) (2016) 3081–3093.
- [21] L. Cardona, R. Araújo, R. Sanchez, Thermo-mechanical characterization of PHB/ PCL blend incorporated with carbon nanotubes, Express Polym. Lett. 19 (2025) 862–877.
- [22] S. Grishchuk, O. Gryshchuk, M. Weber, J. Karger-Kocsis, Structure and toughness of polyethersulfone (PESU)-Modified anhydride-cured tetrafunctional epoxy resin: effect of PESU molecular mass, J. Appl. Polym. Sci. 123 (2) (2012) 1193–1200.
- [23] S.K. Siddhamalli, Toughening of epoxy/polycaprolactone composites via reaction induced phase separation, Polym. Compos. 21 (5) (2000) 846–855.

- [24] S.-E. Lee, E. Jeong, M.Y. Lee, M.-K. Lee, Y.-S. Lee, Improvement of the mechanical and thermal properties of polyethersulfone-modified epoxy composites, J. Ind. Eng. Chem. 33 (2016) 73–79.
- [25] C. Qu, X. Li, Z. Yang, X. Zhang, T. Wang, Q. Wang, et al., Damping, thermal, and mechanical performances of a novel semi-interpenetrating polymer networks based on polyimide/epoxy, J. Appl. Polym. Sci. 136 (41) (2019) 48032.
- [26] J. Liu, W. Fan, G. Lu, D. Zhou, Z. Wang, J. Yan, Semi-interpenetrating polymer networks based on cyanate ester and highly soluble thermoplastic polyimide, Polymers (2019).
- [27] H. Nakanishi, N. Namikawa, T. Norisuye, Q. Tran-Cong-Miyata, Autocatalytic phase separation and graded co-continuous morphology generated by photocuring, Soft Matter 2 (2) (2006) 149–156.
- [28] S. Ali, Z. Khatri, K.W. Oh, I.-S. Kim, S.H. Kim, Preparation and characterization of hybrid polycaprolactone/cellulose ultrafine fibers via electrospinning, Macromol. Res. 22 (5) (2014) 562–568.
- [29] M. Gümüşderelioğlu, S. Dalkıranoğlu, R.S. Aydın, S. Cakmak, A novel dermal substitute based on biofunctionalized electrospun PCL nanofibrous matrix, J. Biomed. Mater. Res., Part A 98 (3) (2011) 461–472.
- [30] C.A. Ramírez-Herrera, I. Cruz-Cruz, I.H. Jiménez-Cedeño, O. Martínez-Romero, A. Elías-Zúñiga, Influence of the epoxy resin process parameters on the mechanical properties of produced bidirectional [±45°] carbon/epoxy woven composites, Polymers (2021).
- [31] I.J. Fernandes, R.V. Santos, E.C.A. dos Santos, T. Rocha, N.S. Domingues, C.A. M. Moraes, Replacement of commercial silica by rice husk ash in epoxy composites: a comparative analysis, Materials Res-IBERO-American J. Mater. 21 (3) (2018).
- [32] X. Qin, D. Wu, Effect of different solvents on poly(caprolactone) (PCL) electrospun nonwoven membranes, J. Therm. Anal. Calorim. 107 (3) (2012) 1007–1013.
- [33] E. Altun, J. Ahmed, M. Onur Aydogdu, A. Harker, M. Edirisinghe, The effect of solvent and pressure on polycaprolactone solutions for particle and fibre formation, Eur. Polym. J. 173 (2022) 111300.
- [34] O. Gryshchuk, J. Karger-Kocsis, Nanostructure in hybrid thermosets with interpenetrating networks and its effect on properties, J. Nanosci. Nanotechnol. 6 (2) (2006) 345–351.
- [35] Y.S. Lipatov, Hybrid binders in polymer composites, Peculiarities of structure and properties conditioned by microphase separation 57 (11) (1985) 1691–1700.
- [36] Y.S. Lipatov, V.F. Rosovitskii, P.V. Datsko, Y.V. Maslak, Dependence of the viscoelastic properties on the degree of segregation of the components in mutually penetrating polymer networks, Mech. Compos. Mater. 23 (6) (1988) 782–786.
- [37] Y.S. Lipatov, Peculiarities of self-organization in the production of interpenetrating polymer networks, J. Macromol. Sci., Part C 30 (2) (1990) 209–232.
- [38] B. Magyar, T. Czigany, G. Szebényi, Metal-alike polymer composites: the effect of inter-layer content on the pseudo-ductile behaviour of carbon fibre/epoxy resin materials, Compos. Sci. Technol. 215 (2021) 109002.
- [39] G. Szebényi, B. Magyar, T. Czigany, Achieving pseudo-ductile behavior of carbon fiber reinforced polymer composites via interfacial engineering, Adv. Eng. Mater. 23 (2) (2021) 2000822.
- [40] Magyar B, Czigány T, Török D, Marton GZ, Balogh F, Szebényi G. Modeling of the healing process of polycaprolactone-interleaved carbon fiber–reinforced composites. Polym. Compos. n/a(n/a).